JGR Space Physics

RESEARCH ARTICLE
10.1029/2019JA027035

One-Year Analysis of Dust Impact-Like Events Onto the MMS Spacecraft

Jakub Vaverka[1], Jiří Pavlů[1], Libor Nouzák[1], Jana Šafránková[1], Zdeněk Němeček[1], Ingrid Mann[2], Shengyi Ye[3], and Per-Arne Lindqvist[4]

[1]Faculty of Mathematics and Physics, Charles University, Prague, Czech Republic, [2]Department of Physics and Technology, The Arctic University of Norway, Tromsø, Norway, [3]Department of Physics and Astronomy, University of Iowa, Iowa City, IA, USA, [4]Department of Space and Plasma Physics, KTH Royal Institute of Technology, Stockholm, Sweden

Key Points:
- Simultaneous dust impact detection by multiple electric field antennas in the monopole and dipole configurations
- Estimation of the dust flux
- Identification of possible sources of the signal misinterpretation

Correspondence to:
J. Vaverka,
jakubvaverka@gmail.com

Citation:
Vaverka, J., Pavlu, J., Nouzá, L. k., Safrankova, J., Nemecek, Z., Mann, I. B., et al. (2019). One-year analysis of dust impact-like events onto the MMS spacecraft. *Journal of Geophysical Research: Space Physics*, *124*. https://doi.org/10.1029/2019JA027035

Received 13 JUN 2019
Accepted 23 SEP 2019
Accepted article online 16 OCT 2019

Abstract We present an analysis of 1-year data of dust impacts observed on two of the Earth-orbiting Magnetospheric Multiscale mission (MMS) spacecraft. The dust impact signals were identified in observations of the electric field probes and were registered simultaneously by monopole and dipole configurations of the instrument. This unique setup allows us to reliably identify changes in the spacecraft potential as candidates for dust impacts. We present a detailed study of the properties of the pulses generated by the dust impacts and show the influence of the local plasma environment (spacecraft location in the Earth magnetosphere) on signals generated by dust impacts and their detection. We discuss the credibility of impact identification and possible sources of signal misinterpretation. We find a total of 784 observed events that we can interpret as dust impacts and that we use to derive a dust flux. We show that MMS1 registered 0.7 and MMS3 0.8 dust impact-like events per hour. This corresponds to dust flux of $2.5–6 \times 10^{-5}$ m^{-2} s^{-1}.

1. Introduction

It has been shown that dust impacts on the spacecraft body can generate pulses in the electric field measurements. Such surprising pulses have been detected for the first time by the Voyager spacecraft during a crossing of Saturn's ring plane (Aubier et al., 1983; Gurnett et al., 1983). This method is recently used for dust detection by many missions in various parts of our solar system such as Deep Space 1 (Tsurutani et al., 2004), Cassini (Kurth et al., 2006; Wang et al., 2006; Ye et al., 2014, 2016), Wind (Malaspina & Wilson, 2016; Malaspina et al., 2014; Wood et al., 2015), Solar Terrestrial Relations Observatory (STEREO; ; Meyer-Vernet et al., 2009; Kellogg et al., 2016; Malaspina et al., 2015; O'Shea et al., 2017; Zaslavsky, 2015; Zaslavsky et al., 2012), Mars Atmosphere and Volatile EvolutioN (Andersson et al., 2015), Cluster (Vaverka et al., 2017a, 2017b), and Magnetospheric Multiscale mission (MMS; Vaverka et al., 2018). The signatures of dust impacts on a spacecraft body are intensively studied also in laboratories (Collette et al., 2016, 2013, 2014, 2015; Dietzel et al., 1973; McBride & McDonnell, 1999; Nouzák et al., 2018) and by computer simulations (Fletcher et al., 2015; Pantellini et al., 2012).

This method has two main advantages with respect to dedicated dust detectors. Many more of the scientific spacecraft are equipped with the electric field instruments than with conventional dust detectors. This gives us an interesting opportunity to obtain some information about dust grains from regions where no missions are focused primarily on dust detection. Another advantage of this technique is that the whole spacecraft body is used as a dust detector and it provides a significantly larger detection area than that of dedicated dust instrument. On the other hand, the disadvantage of such method is that there is nearly no information about the impacting grain and that this method is still not fully understood. A frequently neglected problem is the identification of dust impacts in obtained waveforms. There is an open discussion if all events attributed to dust impacts detected by the STEREO spacecraft are really generated by dust (Kellogg et al., 2018). The reliable answer to this question is very important for future use of the electric field instrument as ordinary dust detectors. O'Shea et al. (2017) presented a complexity of signal detected by the STEREO spacecraft and let several open questions about the detected signal. A large database of dust impacts registered by the Wind spacecraft divided detected pulses into four different categories without proper explanation of their shape (Malaspina & Wilson, 2016). The reliable identification of dust impacts is very important for

the results obtained by this method. The presence of similar signals of different origin complicates dust detection. For example, solitary waves can be easily misinterpreted as dust impacts by some dust detection algorithms when only one electric field antenna/probe is used (Vaverka et al., 2018). Similar pulses can also be generated by instrumental electronics. The example is the Wide Band Data instrument (Gurnett et al., 1997) onboard the Cluster spacecraft, which generates pulses in the electric field data during switching a level of an automatic gain control (Vaverka et al., 2017a). It should be mentioned that higher sampling rates can help with signal identifications.

We use data from the MMS spacecraft because they provide electric field measurements by multiple probes simultaneously in monopole and dipole configurations allowing us to distinguish pulses in the spacecraft potential (candidates for dust impacts) from pulses connected to the ambient electric field as, for example, solitary waves. We analyze shapes, durations, and amplitudes of detected pulses and influence of the ambient plasma on the detected signal. The dust flux is derived from the occurrence rate of pulses attributed to dust impacts.

2. Detection of Dust Impacts

The general understanding of a signal generation by dust impacts can be described as follows. The impact of a dust grain onto the spacecraft body generates an impact plasma cloud (free electrons and ions). These charged particles are influenced by the potential of the spacecraft body and can be subsequently attracted to/repulsed from the spacecraft according to its surface potential (positively charged surface attracts electrons, repulses ions, and vice versa). The interaction of impact cloud particles with the spacecraft body results in fast change of its potential followed by relaxation to the equilibrium value due to the ambient plasma and solar ultraviolet radiation. Such potential changes can be detected by the electric field instruments operating in the monopole configuration where the electric field is measured as a potential drop between one electric probe and the spacecraft body.

The amplitude of the detected signal is thus given by the amount of the released particles which depends on the velocity and mass of impacting grains (Collette et al., 2014; Dietzel et al., 1973; McBride & McDonnell, 1999). The rising time of the pulse is given by the dynamics of the impact cloud (Meyer-Vernet et al., 2017). The recorded rising edge of the pulse can be strongly influenced by the instrumental electronic as well as by sampling frequency of the electric field measurement because corresponding processes typically takes only a few microseconds. The relaxation part of the pulse is given by the parameters of ambient plasma and intensity of photoemission that depends on the distance from the Sun (Zaslavsky, 2015). Environments with high plasma density (magnetosphere of planets) and strong photoemission can significantly reduce the pulse duration and even its amplitude (Vaverka et al., 2017b). Note that the typical duration of the dust impact signature is in the range of milliseconds. Therefore, only instruments with the sampling frequency higher than several kilohertz are able to register dust impact signatures. The configuration of the electric field antennas is very important for dust impact detection. Only instruments operating in the monopole configuration are able to directly register changes of the spacecraft potential (Meyer-Vernet et al., 2014; Ye et al., 2014, 2016). Dipole instruments can detect only direct dust impacts on one of the antennas, events when the expanding impact plasma cloud affects a potential of one antenna boom, or when the spacecraft potential influences dipole antennas in an asymmetrical way. This fact is important to keep in mind during data analysis. The mechanism of the signal generation by dust impacts and its detection by the electric field instruments is described in more details, for example, in Zaslavsky (2015), Meyer-Vernet et al. (2017), and Vaverka et al. (2017a, 2018).

3. MMS Spacecraft

The four MMS spacecraft are orbiting the Earth in close formation since 2015 (Burch et al., 2016). MMS crosses various parts of the Earth's magnetosphere on their highly elliptical orbit. This allows us to study dust impacts in different plasma environments. Each of these spacecraft is equipped with three pairs of electric field probes, two in the spin plane (Probes P1–P4 [120 m tip-to-tip; Lindqvist et al., 2016; Torbert et al., 2016]) and one in the axial plane (Probes P5 and P6 [29 m; Ergun et al., 2016; Torbert et al., 2016]). The advantage of this instrument for possible dust impact detection is that it operates nearly simultaneously in the monopole and dipole configurations. In the monopole configuration, the probe-to-spacecraft potential is measured for all six probes but only three of them are transmitted to the ground, one from each pair ($P1$, $P3$, and $P5$).

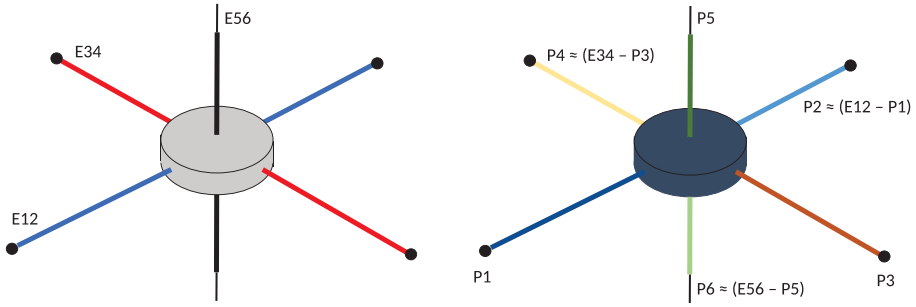

Figure 1. A simplified sketch of the electric field instrument for both operating modes, dipole (left) and monopole (right), and corresponding color scheme used in this paper.

This is followed by the electric field measurement (dipole configuration) as a potential drop between two probes on opposite booms ($E12$, $E34$, and $E56$). The probe-to-spacecraft potentials for the rest of the probes ($P2$, $P4$, and $P6$) can be derived from previous measurements. Figure 1 shows the probes configuration for both modes (dipole left and monopole right), corresponding color scheme is later used in Figure 2. The monopole configuration is sensitive to changes of the spacecraft potential, while the dipole configuration is mainly sensitive to changes in the ambient electric field or to changes in the potential of dipole antennas. This unique measurement allows us to reliably distinguish changes in the spacecraft potential (candidates for dust impacts) from other signal related to changes in the ambient plasma or in the electric field. These signals could be easily misinterpreted as dust impacts (Vaverka et al., 2018).

Only tips of the electric field instrument booms are used as potential sensors (probes). The tips are spheres (8-cm diameter) for spin plane double probes and tubes (1-m long and 0.64-cm diameter) for axial probes. Influence of the expanding plasma cloud and asymmetrical spacecraft potential is smaller than for observations in dipole configuration made on other spacecraft as Wind, STEREO, and Cassini. The negative current bias is used for probes to reduce their high positive potential in tenuous plasma and to reduce the dependence of the probe voltage on fluctuations of the plasma electron current (Lindqvist et al., 2016). This means that the floating potential of the probe is closer to 0 (plasma potential) than the potential of the spacecraft body (but still positive). The monopole measurements (probe-to-spacecraft potential difference) can be used to estimate the spacecraft potential and to monitor the ambient electron flux (Andriopoulou et al., 2018; Pedersen et al., 2008). The potential of the Earth-orbiting spacecraft is given by the balance of the electron collection current and photoemission current. The spacecraft is thus charged positively in this case. Variations of plasma density for different parts of the Earth magnetosphere and solar wind conditions result in the different values of the positive spacecraft potential from a few volts in the solar wind up to tens of volts for environments with a low plasma density as the plasma sheet and tail lobes (Vaverka et al., 2017b).

The sampling frequency is a very important parameter for dust impact detection. The MMS electric field instrument can operate with different sampling modes: Slow (8 s^{-1}), Fast (32 s^{-1}), Burst (up to 16,384 s^{-1}), and Hight Rate Burst (up to 262,144 s^{-1}). Only Burst modes are fast enough for the dust impact detection. We use only data in the Burst mode for the analysis presented in this paper. A typical operation time in this mode slightly exceeds 1 hr/day.

4. Events Identification

It is generally a challenging issue to select events related to dust impacts from the electric field data mainly in environments where natural waves such as solitary waves are present in large numbers. We used the fact that the electric field instrument onboard the MMS spacecraft operates simultaneously in the monopole and dipole configuration. It has been mentioned above that hypervelocity dust impacts on the spacecraft body can generate short pulses in the spacecraft potential. Such changes can be detected by the electric field instrument operating in the monopole configuration (probe-to-spacecraft potential measurement). In this case, all monopole probes should register identical signals with the same polarity independently of their geometrical orientation. For the dipole configuration, on the other hand, dust impacts on the spacecraft body only generate a signal when the expanding cloud affects the potential of the electric probe or when the spacecraft potential influences dipole probes in an asymmetrical way. We use data from multiple electric field instruments in the monopole and dipole configuration for reliable identification of the changes in the

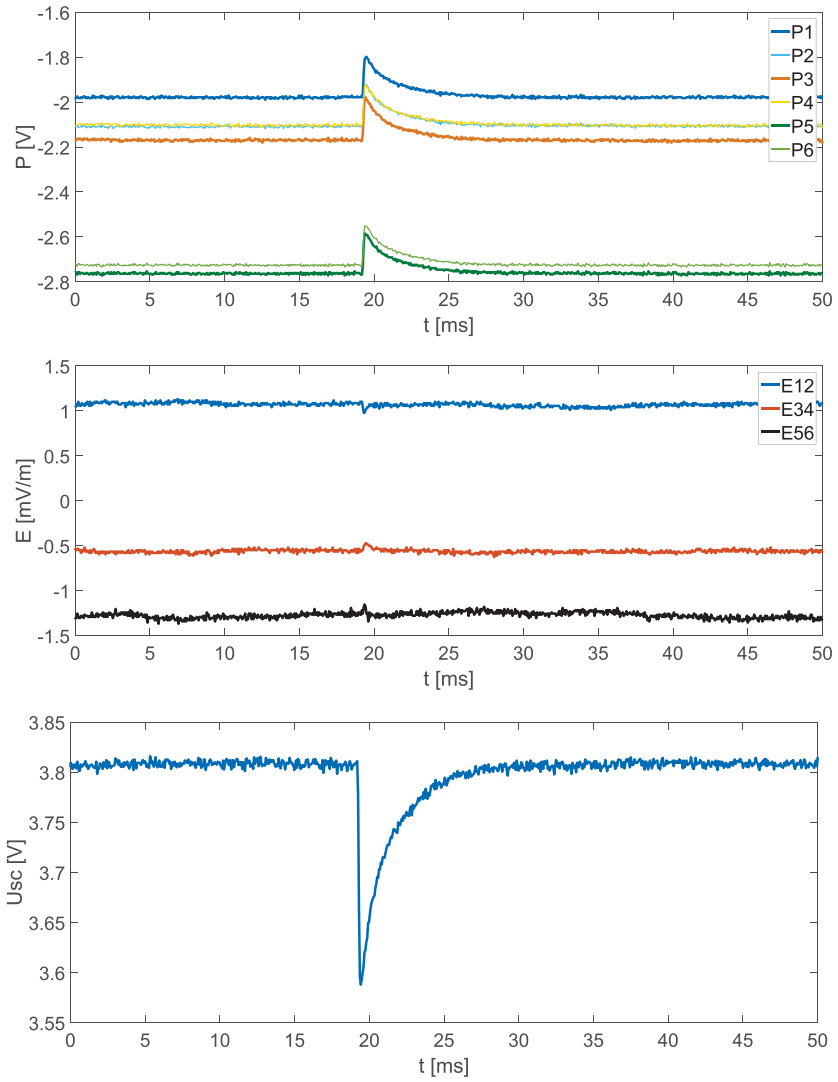

Figure 2. The example of a typical event related to the change of the spacecraft potential (candidate for a dust impact) selected by the automatic code. Probe-to-spacecraft potential measurement, *P* (top), the electric field measurement in dipole configuration, *E* (middle), and the spacecraft potential, U_{SC} (bottom).

spacecraft potential (candidates for dust impacts). The difference between structures in the ambient electric field like solitary waves and the changes in the spacecraft potential detected by the electric field instrument onboard the MMS spacecraft are described in detail in Vaverka et al. (2018). Our event selection process can be described in the following three steps: (1) preselection of interesting events, (2) identification of events related to changes in the spacecraft potential, and (3) visual inspection.

1. In the first step, the automatic code selected events for which the derivative of the spacecraft potential (derived from the monopole measurements) exceeded predefined threshold (20 mV).
2. These preselected events were tested, if the signal from monopole antennas corresponds to a change in the spacecraft potential. Practically, correlation coefficients for signals from two opposite monopole probes were calculated for both spin plane double probes (*P*1-*P*2 and *P*3-*P*4) for 3 ms of data (1 ms before and 2 ms after the strongest derivation in the spacecraft potential). Events with both correlation coefficients exceeding 0.9 were saved as potential candidates for dust impacts. This step effectively eliminated all pulses related to changes in the ambient plasma or electric field as solitary waves. The correlation coefficients for such events should be close to −1 (monopole probes on the same axes detect an identical signal with the opposite polarity). In the magnetosphere, this step significantly reduced the number of events, because the number of solitary waves greatly exceeds the number of expected dust impacts (Pickett et al., 2004).

3. As the last step, all events selected by this method were visually inspected (monopole and dipole data) to prevent unexpected signals corrupting the results.

A typical event selected with this procedure is shown in Figure 2. The top panel shows the probe-to-spacecraft potential for all probes (monopoles), P, the middle panel shows the electric field, E, and the bottom panel shows the spacecraft potential derived from the monopole data, U_{SC}. The colors used in this figure correspond to the color scheme in Figure 1. One can see that all pulses in probe-to-spacecraft potential measurements are identical (the correlation coefficients for probes $P1$-$P2$ and $P3$-$P4$ are close to unity). Moreover, the dipole data in the middle panel show none or very small pulses. Such signals can only be explained by a change in the spacecraft potential, which is shown in the bottom panel of Figure 2. This procedure was applied to 1-year data (2016) from two MMS spacecraft (MMS1 and MMS3), and the results are discussed below. The measured waveforms contain also a different kind of pulses. Waveforms from the MMS2 spacecraft contain pulses related to the operation of Electron Drift Instrument (Torbert et al., 2016). This is a reason why we used data from the MMS3 instead of MMS2.

5. Observations

We have identified (in MMS1 and MMS3 monopole data) 784 events corresponding to fast reduction of the positive spacecraft potential, which could be generated by dust impacts. We now consider the pulse shapes, amplitudes, and count rates.

5.1. Shape of the Pulses

A very important fact is that the shapes of detected pulses are not identical. The pulses related to the changes in the spacecraft potential vary from sharp short spikes to round longer pulses. Three different examples of pulses in the spacecraft potential, U_{SC} are shown in Figure 3. We have detected variety of pulses from the sharp, shown in the top panel, to the long one from the bottom panel of Figure 3. The duration and the shape (sharp/round) of pulses depend on U_{SC}. The pulses are short and sharp for low values of the spacecraft potentials and longer and round for higher spacecraft potentials. This behavior is shown in Figure 4 for 363 pulses detected by MMS1. The left panel shows the duration of the pulse, t, as a function of U_{SC}. The duration t, is defined as a time when the amplitude of the pulse is reduced to $1/e$ of the maximal value. Pulse duration depends on U_{SC} and increases from less than 1 ms for low spacecraft potentials up to 20 ms for events when the spacecraft potential reached 35 V. It has been mentioned above that the equilibrium spacecraft potential depends on the ambient plasma parameters, mainly on the electron density. The fact that the duration (relaxation) of the pulses depends on the spacecraft potential thus simply means that the detected pulses are longer in the tenuous plasma (higher spacecraft potential) and currents returning the spacecraft potential back to its equilibrium value are stronger in the dense plasma (lower positive potential; Vaverka et al., 2017b). The dependence of the pulse duration on the ambient plasma conditions has been observed also by the Cassini spacecraft during the Grand Finale orbits (Ye et al., 2018). The fact that the relaxation time depends on the plasma density supports the hypotheses that these signals are connected to changes in the spacecraft potential and excludes a possibility that these pulses are generated in the instrumental electronics because such pulses should be independent on the ambient plasma parameters.

The right panel of Figure 4 shows the time needed to reach the maximum value of the pulse, t_{max}, as a function of the spacecraft potential, U_{SC}. This parameter also describes the shape of the pulses—time is short for sharp spikes and significantly longer for round pulses as shown in the last panel of Figure 3. The explanation of the various shapes of the pulses can be connected to the signal generation by dust impacts. If the plasma density is large enough, the relaxation part of the pulse becomes dominant even before the pulse can reach its maximum. This is the reason why sharp pulses shown in the top panel of Figure 3 occur in environments with the high plasma density. The amplitude of the pulses can be reduced in this case (Vaverka et al., 2017b). The discharging current becomes smaller with increasing equilibrium spacecraft potential (decreasing plasma density) and the pulse can reach its maximum before the relaxation process starts to dominate. The rising part of the pulse is given by particles (ions) escaping from the spacecraft (Meyer-Vernet et al., 2017). The distance, when the escaping particles are far enough that their influence on the spacecraft potential is negligible, depends on the ambient plasma density (Debye length). Escaping ions have to get further from the spacecraft in the low-density plasma to lose their influence on the spacecraft potential. This takes longer, if we assume the same velocity of the expanding ions. The theory presented by Meyer-Vernet et al. (2017) for signal generation by dust impacts and consequent ion cloud expansion is

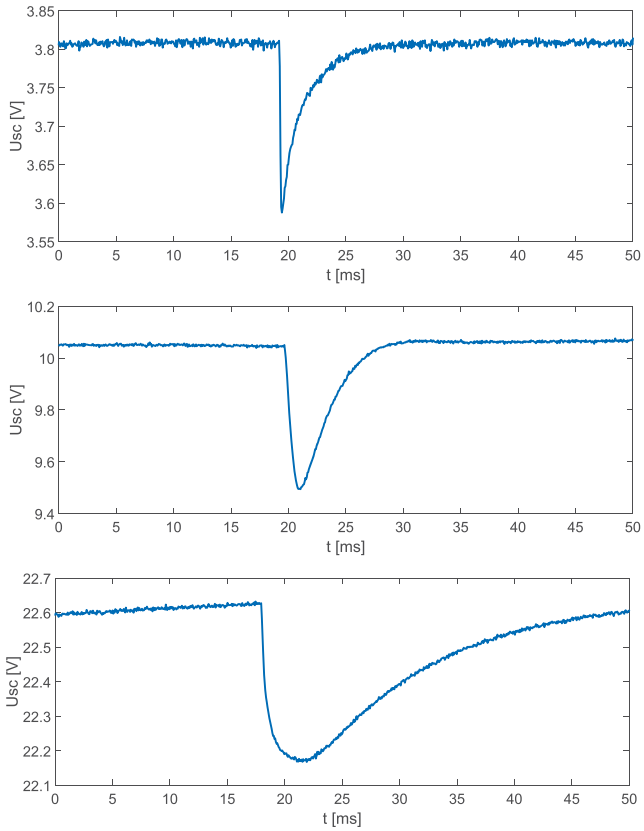

Figure 3. Examples of three different pulses in the spacecraft potential (candidates for dust impacts).

relatively complex, but the pulse rising times between 0.2 and 5 ms are in a good agreement with this model for Earth magnetosphere conditions. This supports our hypothesis that expansion of ion cloud generated by dust impacts can be responsible for these events.

5.2. Amplitudes of the Pulse

The detected pulses show a large variety in their amplitudes. We have detected pulses from 0.05 (detection limit) up to 27 V. The amplitude depends on the velocity and mass of the impacting grains (Collette et al., 2014; Dietzel et al., 1973; McBride & McDonnell, 1999). The amplitude strongly increases with the velocity (power ranges from 3.8 to 4.2; Collette et al., 2014) and linearly with mass (power of 3 in size). The fact that impacts of smaller dust grains are much more probable than impacts of bigger ones (Grün et al., 1985) implies that we should expect much more events with small amplitudes for events related to the dust impact.

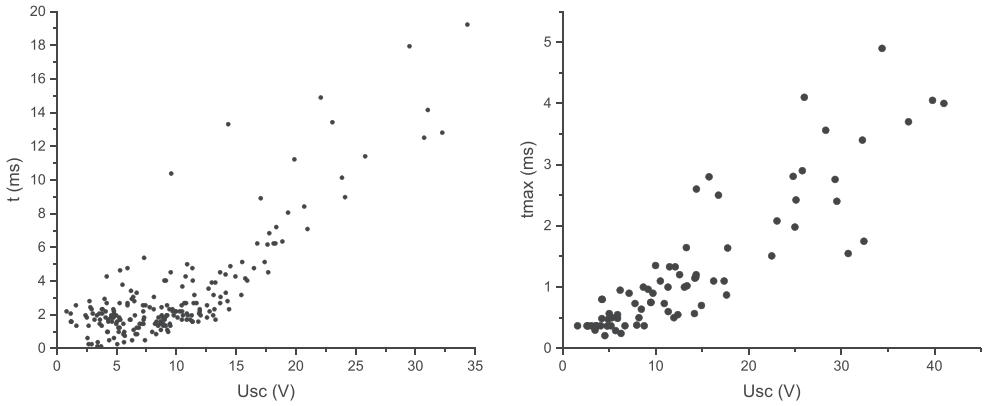

Figure 4. The duration of the pulse (left panel) and the time needed to reached the peak of the pulse (right panel) as a function of the spacecraft potential.

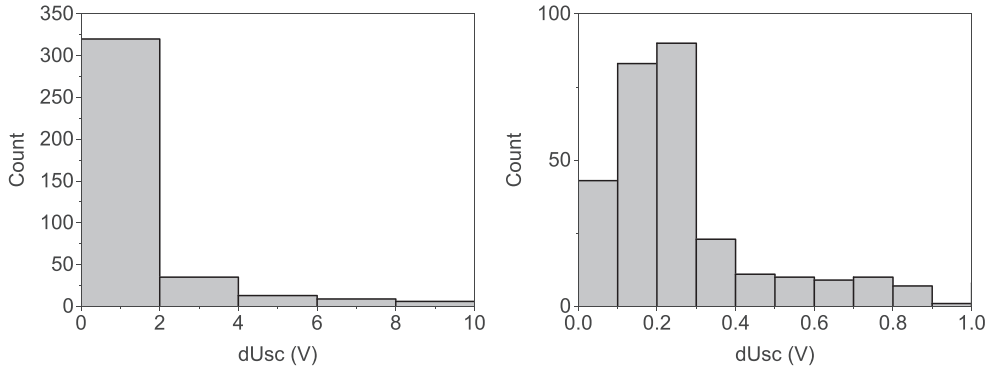

Figure 5. Histograms of the amplitudes of the pulses detected by the Magnetospheric Multiscale mission 1 spacecraft in 2016 with a bin size 2 V (left panel) and 100 mV (right panel).

Figure 5 shows two histograms of pulse amplitudes detected by the MMS1 spacecraft. The left panel shows a histogram with a bin size of 2 V, and the right panel shows a detail of the same data with a bin size of 100 mV. It is possible to see that the pulses with higher amplitudes are less frequent than smaller ones and it is in a good agreement with the assumption that the pulses are generated by the dust impacts. It is important to note that this is not a proof that the dust impacts are responsible for these signals. The figure shows that the majority of the events is smaller than 2 V and that the larger events are very sporadic. The detailed picture (right panel) shows that the large portion of events has amplitudes close to 200‘mV and that the number of events decreases for amplitudes smaller than 200 mV. The sensitivity of the detection method is limited and depends on the background signal (presence of electromagnetic waves). It is important to note that electromagnetic waves can be very intens in some regions. In these cases, the ability to detect dust impacts is significantly reduced. Pulses close to 50 mV are at the detection limit of our method, on the other hand, according to our experience, it should be possible to detected pulses larger than 100 mV in most of the time. There should be no reason to detect less pulses between 100 and 200 mV than between 200 and 300 mV. The possible explanation could be that some of the pulses close to 200 mV are not related to the dust impacts. Another explanation is that we overestimated the sensitivity and not all events larger than 100 mV are registered.

Figure 6 shows amplitudes of the detected pulses as a function of the spacecraft potential (ambient plasma density). The right panel shows a detail focused on events smaller than 1 V. It is possible to see that amplitudes of pulses are limited by the spacecraft potential. We have never detected pulse larger than the actual spacecraft potential that means that the spacecraft potential never changed its polarity from positive to negative. The typical potential of the MMS spacecraft is between 4 and 15 V. Note that the Active Spacecraft Potential Control (ASPOC) instrument reduces the spacecraft potential into this range when the spacecraft cross regions with low plasma density (Torkar et al., 2016). We have detected few pulses higher than 20 V

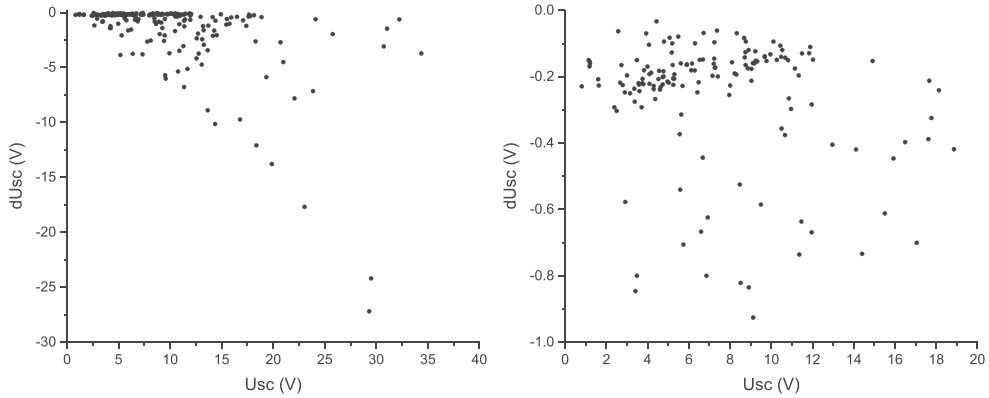

Figure 6. Amplitudes of the detected pulses as a function of the spacecraft potential (left) with a detail for a small events (right).

despite the fact that the spacecraft potential higher than 20 V is very atypical. The right panel of Figure 6 shows an increased amount of pulses with amplitudes close to the 200 mV as shown in the left panel of Figure 5. Another possible explanation for this increase can be that for low values of the spacecraft potential (dense ambient plasma or activity of the ASPOC instrument) are amplitudes of the pulses reduced to the detection limit by the stronger currents pushing the spacecraft potential back to the equilibrium value as shown in the top panel of Figure 3.

5.3. Count Rate

We have analyzed 1 year of data for two of MMS spacecraft (MMS1 and MMS3) to be sure that the detected events are not related only to one of the spacecraft. The operation time in the burst mode is 522.5 hr for MMS1 and 513.8 hr for MMS3 during the whole 2016 year. Figure 7 shows the amount of all detected pulses by MMS1 and MMS 3 (left) and corresponding count rates for each month. The average detected count rate is 0.7 events per hour for MMS1 and 0.8 events per hour for MMS 3. These values are relatively constant over the year. A small fluctuation can be a result of a limited amount of pulses in the individual months. It is important to note that the yearly modulation of interstellar dust flux (peaking in March) has been reported by Zaslavsky et al. (2012), Malaspina et al. (2014), and Kellogg et al. (2016). It can be possible that this effect is hidden in the fluctuations caused by a limited amount of pulses in the individual months. The sensitivity of dust detection can be variable over the year because the data comes dominantly from different regions (solar wind vs. Earth's magnetosphere) in various months. The statistics can be also corrupted if some of the events are not generated by dust impacts. The fact that we detect a similar amount of events by both spacecraft shows that the pulses are not result of any technical issue on the single spacecraft. On the other hand, these spacecraft are identical and similar amount of events registered by both spacecraft could be a result of identical constructions.

In the case that all events are triggered by dust impacts, the derived dust flux is in range from $2.5 \times 10^{-5}$to 6 $\times 10^{-5}$ m^{-2} s^{-1} and it strongly depends on the effective cross section of the spacecraft which depends on the preferred direction of incoming grains. The effective cross section is 3 m^2 for the grains coming from the side (equatorial plane) and 7 m^2 for the grains coming from the top/bottom. Obtained dust flux according to the interplanetary dust flux model (Grün et al., 1985) corresponds to impacts of dust grains heavier than 10^{-12} g (3.4 10^{-5} m^{-2} s^{-1}). The grain of this mass (approximately 1 μm in diameter) impacting with the velocity 20 km/s or higher can generate pulses above our detection limit (Collette et al., 2014). This shows that the flux of interplanetary dust can explain the amount of the pulses we detected. Detected dust flux is in a similar range as values presented by Zaslavsky et al. (2012) for β-Meteoroids (1–6 $\times 10^{-5}$ m^{-2} s^{-1}) and interstelar dust (2–10 $\times 10^{-5}$ m^{-2} s^{-1}) detected by STEREO.

5.4. Positive Events

A very surprising fact is that we have detected pulses with the opposite polarity (than events described above) 279 by MMS1 and 367 by MMS3. The positive spacecraft potential becomes more positive for a short time and returns back to the equilibrium value as previous pulses during these events. The monopole and dipole data

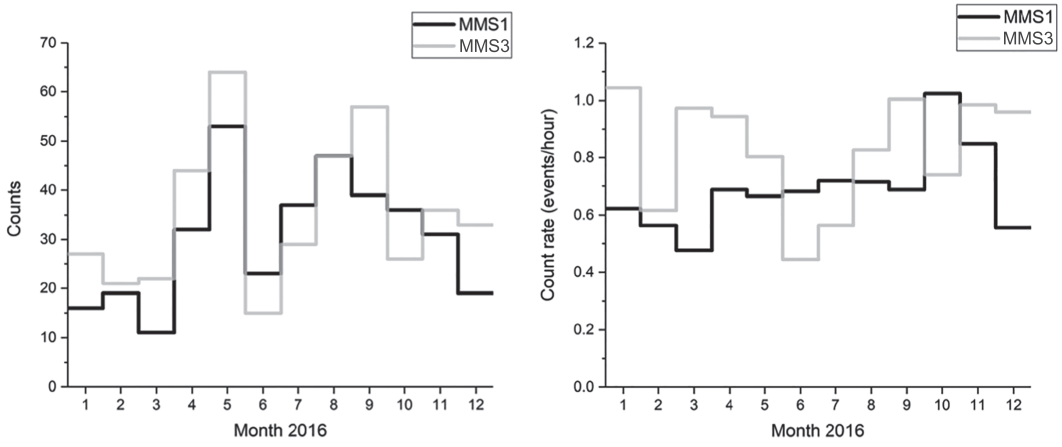

Figure 7. The amount of detected pulses by MMS1 and MMS3 (left panel) and corresponding count rates for each month of 2016 (right panel). MMS = Magnetospheric Multiscale mission.

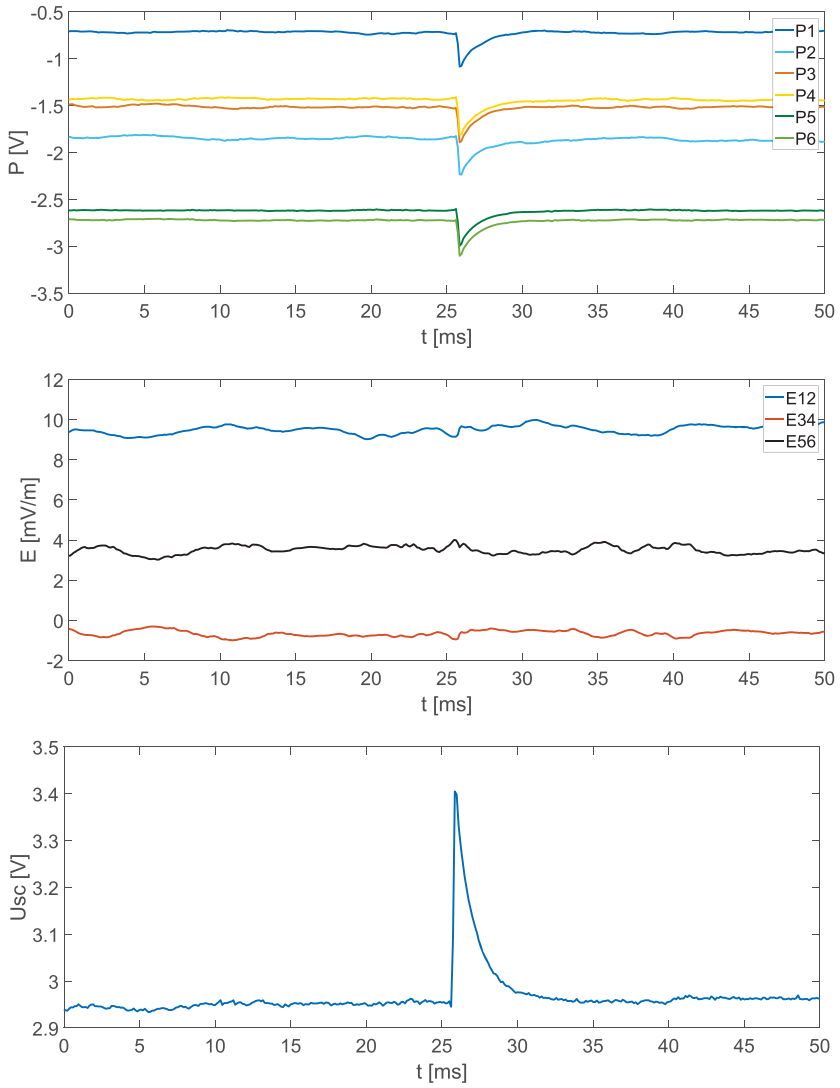

Figure 8. An example of the event with opposite polarity. Probe-to-spacecraft potential measurement, P (top), the electric field measurement in dipole configuration, E (middle), and the spacecraft potential, U_{SC} (bottom).

show exactly the same behavior as in Figure 2 but with the opposite polarity. One example of the pulse with opposite polarity is shown in Figure 8. The existence of such inverted pulses has been also reported by O'Shea et al. (2017) from the STEREO spacecraft without satisfactory explanation of their origin. It is not easy to find a process which can be responsible for such behavior and make the positive spacecraft potential even more positive. There is no mechanism related to dust impacts which can generate such pulses. Hypothetically, a slow impact of a positively charged dust grain could result in the collection of the positive charge without a generation of impact plasma. This event could cause a similar spike with the opposite polarity. On the other hand, the amplitude of such pulse will be much smaller than the amplitude of detected spikes because the amount of the positive charge carried by a dust grain is to small to increase the spacecraft potential by about hundreds of millivolts. Interesting properties of these events are shown in Figure 9. Amplitude of the pulse, dU_{SC}, as a function of the spacecraft potential, U_{SC}, (left panel) shows a very interesting fact that the amplitude of the pulses is strictly connected to the spacecraft potential. This behavior is totally different than for pulses described before (compare a left panel of Figure 9 with Figure 6). The fact that the size of the pulses is given by the spacecraft potential suggests that these events are probably generated artificially (the amplitude should depend on the velocity and size of impacting grains in a case when the signal is generated by dust impacts). The amplitude of such pulses decreases with the spacecraft potential and we have not detected any positive pulses for the spacecraft potential higher than 17 V contrary to the negative

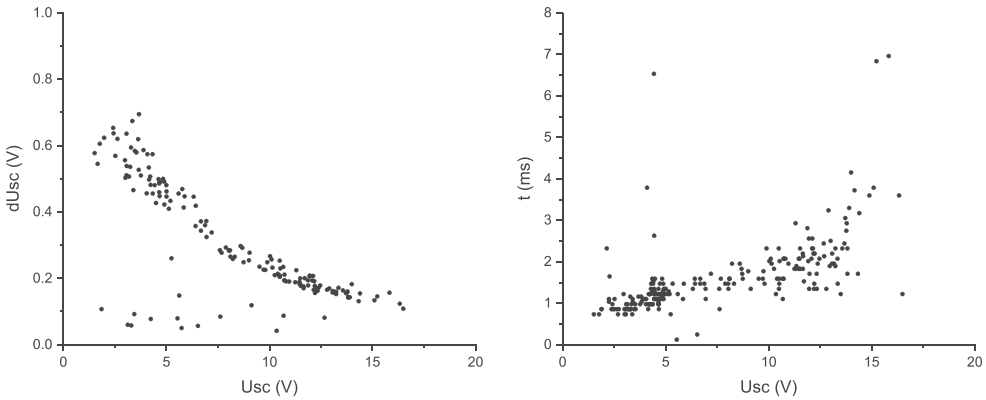

Figure 9. Amplitude (left) and duration (right) of the positive (inverted) pulses.

pulses described above (candidates for dust impacts). The right panel of Figure 9 shows that the duration of the pulses depends on the spacecraft potential (plasma density) in the same way as for the negative spikes (compare with the left panel of Figure 4). This shows that these pulses are also probably related to changes in the spacecraft potential. The different amplitude dependence on the spacecraft potential suggests that the positive and negative pulses are of different origin. However, some of the negative spikes (candidates for dust impacts) can be generated by the same unknown mechanism as the positive spikes. It is not possible to misinterpret these positive events as dust impacts. On the other hand, the existence of such events with unknown origin opens the important question if some events interpreted as dust impacts could be generated also by a different mechanism.

6. Discussion

The pulses in the spacecraft potential (with reduction of the spacecraft potential) detected by the MMS spacecraft are probably generated by dust impacts. There are several supportive indications for this hypothesis:

- The simultaneous monopole and dipole electric field measurements show that these events are related to changes of the spacecraft potential (Figure 2).
- The fact that the duration of these pulses depends on the spacecraft potential (ambient plasma density) also suggests that these pulses are related to changes of the spacecraft potential. For example, pulses generated in the instrument electronics should be independent on ambient plasma conditions.
- The rising part of the pulse depends on the spacecraft potential (thus on the plasma density in a particular region) and the time needed to reach the maximum of the pulse is similar as predicted by Meyer-Vernet et al. (2017) for ion cloud expansion.
- The pulses are distributed over the year evenly.
- Both spacecraft detected similar amount of the events (MMS1 0.7 events per hour and MMS3 0.8 events per hour). This means that the events are not related to some technical issue on one of the spacecraft.
- There are significantly more pulses with a smaller amplitude than bigger ones. This corresponds to what is expected from the dust flux model.
- Derived dust flux of 2.5–6 $\times$ 10^{-5} m^{-2} s^{-1} corresponds to the expected value for the dust flux model for grains larger than 1 micron (Grün et al., 1985).
- There is no correlation between the operation of active experiments onboard the spacecraft as ASPOC and Electron Drift Instrument. Detected events are not generated by these active experiments.

The existence of the positive pulses in the spacecraft potential of unknown origin shows that there is another mechanism influencing the spacecraft potential. The surprising dependence of pulse amplitude on the spacecraft potential for positive events shows that these events are generated by a different mechanism than negative ones (candidates for dust impacts). However, it is not possible to exclude the possibility that some of the negative pulses can be generated by different processes than by dust impacts.

7. Conclusion

We have detected 784 pulses in the spacecraft potential by the electric field instrument over the year 2016 by two MMS spacecraft. The derived count rates are 0.7 events per hour for MMS1 and 0.8 events per hour for MMS3. This corresponds to the dust flux of 2.5–6 $\times$ 10^{-5} m^{-2} s^{-1}, which is in good agreement with the dust flux model for grains larger than 1 μm (Grün et al., 1985). Several indications show that these events could be generated by dust impacts on the spacecraft body. On the other hand, it is not possible to exclude another origin for these pulses. The presence of the pulses (646) with the opposite polarity and their unknown origin shows a very important fact that dust impact detection by electric field instruments is a very challenging issue even for multiple electric field antennas operating simultaneously in the monopole and dipole configurations. Such configuration allows us to reliably distinguish pulses in the spacecraft potential and signals from the ambient plasma/electric field as solitary waves.

Detection of dust grains in space by the electric field instruments is still a relatively new technique recently used for many spacecraft in various locations in our solar system. Obtained results showed that there is still a need for better understanding of signatures generated by dust impacts, their detection, and identification mainly in environments with low dust impact rate as well as to fully understand all processes generating pulses in the spacecraft potential and in the electric field measurements. Reliable identification of dust impacts is mandatory for establishing this method as an ordinary dust detection technique.

Acknowledgments
This work was supported by Czech Ministry of Education Youth and Sports under Contract LTAUSA 17066 and in part by the Czech Science Foundation under Project 17-06065S. The contribution of S. Y. was supported by NASA CDAP grant (14397000) Understanding Dust Dynamics in Saturn's E-ring Using CDA/RPWS measurements, Modeling and Laboratory Experiments, and I. M. was supported by the Research Council of Norway through Grant 262941. We acknowledge the Magnetospheric MultiScale (MMS) development, operations, and science teams. The data used in this paper were provided by the MMS Science Data Center (https://lasp.colorado.edu/mms/sdc/public/). The authors thank to ISSI (International Space Science Institute) in Bern for organizing of the meeting that discussions within the working group Physics of Dust Impacts: Detection of Cosmic Dust by Spacecraft and its Influence on the Plasma Environment contributed to complementation of this paper.

References

Andersson, L., Weber, T. D., Malaspina, D., Crary, F., Ergun, R. E., Delory, G. T., et al. (2015). Dust observations at orbital altitudes surrounding Mars. *Science*, *350*(6261), aad0398.

Andriopoulou, M., Nakamura, R., Wellenzohn, S., Torkar, K., Baumjohann, W., Torbert, R. B., et al. (2018). Plasma density estimates from spacecraft potential using MMS observations in the dayside magnetosphere. *Journal of Geophysical Research: Space Physics*, *123*, 2620–2629. https://doi.org/10.1002/2017JA025086

Aubier, M. G., MeyerâĂŘVernet, N., & Pedersen, B. M. (1983). Shot noise from grain and particle impacts in Saturn's ring plane. *Geophysical Research Letters*, *10*(1), 5–8.

Burch, J. L., Moore, T. E., Torbert, R. B., & Giles, B. L. (2016). Magnetospheric multiscale overview and science objectives. *Space Science Reviews*, *199*(1-4), 5–21.

Close, S., Linscott, I., Lee, N., Johnson, T., Strauss, D., Goel, A., et al. (2013). Detection of electromagnetic pulses produced by hypervelocity micro particle impact plasmas. *Physics of Plasmas*, *20*(9), 092102.

Collette, A., Grün, E., Malaspina, D., & Sternovsky, Z. (2014). Micrometeoroid impact charge yield for common spacecraft materials. *Journal of Geophysical Research: Space Physics*, *119*, 6019–6026. https://doi.org/10.1002/2014JA020042

Collette, A., Malaspina, D. M., & Sternovsky, Z. (2016). Characteristic temperatures of hypervelocity dust impact plasmas. *Journal of Geophysical Research: Space Physics*, *121*, 8182–8187. https://doi.org/10.1002/2015JA022220

Collette, A., Meyer, G., Malaspina, D., & Sternovsky, Z. (2015). Laboratory investigation of antenna signals from dust impacts on spacecraft. *Journal of Geophysical Research: Space Physics*, *120*, 5298–5305. https://doi.org/10.1002/2015JA021198

Dietzel, H., Eichhorn, G., Fechtig, H., Grun, E., Hoffmann, H.-J., & Kissel, J. (1973). The Heos 2 and Helios micrometeoroid experiments. *Journal of Physics E: Scientific Instruments*, *6*(3), 209–217.

Ergun, R. E., Tucker, S., Westfall, J., Goodrich, K. A., Malaspina, D. M., Summers, D., et al. (2016). The axial double probe and fields signal processing for the MMS mission. *Space Science Reviews*, *199*(1-4), 167–188.

Fletcher, A., Close, S., & Mathias, D. (2015). Simulating plasma production from hypervelocity impacts. *Physics of Plasmas*, *22*(9), 093504.

Grün, E., Zook, H. A., Fechtig, H., & Giese, R. H. (1985). Collisional balance of the meteoritic complex. *Icarus*, *62*(2), 244–272.

Gurnett, D. A., Grün, E., Gallagher, D., Kurth, W. S., & Scarf, F. L. (1983). Micron-sized particles detected near saturn by the Voyager plasma wave instrument. *Icarus*, *53*(2), 236–254.

Gurnett, D. A., Huff, R. L., & Kirchner, D. L. (1997). The wide-band plasma wave investigation. *Space Science Reviews*, *79*(1-2), 195–208.

Kellogg, P. J., Goetz, K., & Monson, S. J. (2016). Dust impact signals on the Wind spacecraft. *Journal of Geophysical Research: Space Physics*, *121*, 966–991. https://doi.org/10.1002/2015JA021124

Kellogg, P. J., Goetz, K., & Monson, S. J. (2018). Are STEREO single hits dust impacts? *Journal of Geophysical Research: Space Physics*, *123*, 7211–7219. https://doi.org/10.1029/2018JA025554

Kurth, W. S., Averkamp, T. F., Gurnett, D. A., & Wang, Z. (2006). Cassini RPWS observations of dust in Saturn's E ring. *Planetary and Space Science*, *54*(9-10), 988–998.

Lindqvist, P., Olsson, G., Torbert, R. B., King, B., Granoff, M., Rau, D., et al. (2016). The spin-plane double probe electric field instrument for MMS. *Space Science Reviews*, *199*(1-4), 137–165.

Malaspina, D. M., Horanyi, M., Zaslavsky, A., Goetz, K., Wilson, L. B., & Kersten, K. (2014). Interplanetary and interstellar dust observed by the Wind/WAVES electric field instrument. *Geophysical Research Letters*, *41*, 266–272. https://doi.org/10.1002/2013GL058786

Malaspina, D. M., O'Brien, L. E., Thayer, F., Sternovsky, Z., & Collette, A. (2015). Revisiting STEREO interplanetary and interstellar dust flux and mass estimates. *Journal of Geophysical Research: Space Physics*, *120*, 6085–6100. https://doi.org/10.1002/2015JA021352

Malaspina, D. M., & Wilson, L. B. III (2016). A database of interplanetary and interstellar dust detected by the Wind spacecraft. *Journal of Geophysical Research: Space Physics*, *121*, 9369–9377. https://doi.org/10.1002/2016JA023209

McBride, N., & McDonnell, J. A. M. (1999). Meteoroid impacts on spacecraft: Sporadics, streams, and the 1999 leonids. *Planetary and Space Science*, *47*(8-9), 1005–1013.

Meyer-Vernet, N., Maksimovic, M., Czechowski, A., Mann, I., Zouganelis, I., Goetz, K., et al. (2009). Dust detection by the wave instrument on STEREO: Nanoparticles picked up by the solar wind? *Solar Physics*, *256*(1-2), 463–474.

Meyer-Vernet, N., Moncuquet, M., Issautier, K., & Lecacheux, A. (2014). The importance of monopole antennas for dust observations: Why Wind/WAVES does not detect nanodust. *Geophysical Research Letters*, *41*, 2716–2720. https://doi.org/10.1002/2014GL059988

Meyer-Vernet, N., Moncuquet, M., Issautier, K., & Schippers, P. (2017). Frequency range of dust detection in space with radio and plasma wave receivers: Theory and application to interplanetary nanodust impacts on Cassini. *Journal of Geophysical Research: Space Physics*, *122*, 8–22. https://doi.org/10.1002/2016JA023081

Nouzák, L., Hsu, S., Malaspina, D., Thayer, F. M., Ye, S., Pavlů, J., et al. (2018). Laboratory modeling of dust impact detection by the Cassini spacecraft. *Planetary and Space Science*, *156*, 85–91.

O'Shea, E., Sternovsky, Z., & Malaspina, D. M. (2017). Interpreting dust impact signals detected by the STEREO spacecraft. *Journal of Geophysical Research: Space Physics*, *122*, 11,864–11,873. https://doi.org/10.1002/2017JA024786

Pantellini, F., Landi, S., Zaslavsky, A., & Meyer-Vernet, N. (2012). On the a spherical plasma cloud turning collisionless: Case of a cloud generated by a nanometre dust grain impact on an uncharged target in space. *Plasma Physics and Controlled Fusion*, *54*(4), 045005. https://doi.org/10.1088/0741-3335/54/4/045005

Pedersen, A., Lybekk, B., André, M., Eriksson, A., Masson, A., Mozer, F. S., et al. (2008). Electron density estimations derived from spacecraft potential measurements on cluster in tenuous plasma regions. *Journal of Geophysical Research*, *113*, A07S33. https://doi.org/10.1029/2007JA012636

Pickett, J. S., Kahler, S. W., Chen, L. ., Huff, R. L., SantolÃŋk, O., Khotyaintsev, Y., et al. (2004). Solitary waves observed in the auroral zone: The Cluster multi-spacecraft perspective. *Nonlinear Processes in Geophysics*, *11*(2), 183–196.

Torbert, R. B., Russell, C. T., Magnes, W., Ergun, R. E., Lindqvist, P., LeContel, O., et al. (2016). The fields instrument suite on MMS: Scientific objectives, measurements, and data products. *Space Science Reviews*, *199*(1-4), 105–135.

Torbert, R. B., Vaith, H., Granoff, M., Widholm, M., Gaidos, J. A., Briggs, B. H., et al. (2016). The Electron Drift Instrument for MMS. *Space Science Reviews*, *199*(1-4), 283–305.

Torkar, K., Nakamura, R., Tajmar, M., Scharlemann, C., Jeszenszky, H., Laky, G., et al. (2016). Active spacecraft potential control investigation. *Space Science Reviews*, *199*(1-4), 515–544.

Tsurutani, B. T., Clay, D. R., Zhang, L. D., Dasgupta, B., Brinza, D., Henry, M., et al. (2004). Plasma clouds associated with comet P/Borrelly dust impacts. *Icarus*, *167*(1), 89–99.

Vaverka, J., Nakamura, T., Kero, J., Mann, I., De Spiegeleer, A., Hamrin, M., et al. (2018). Comparison of dust impact and solitary wave signatures detected by multiple electric field antennas onboard the MMS spacecraft. *Journal of Geophysical Research: Space Physics*, *123*, 6119–6129. https://doi.org/10.1029/2018JA025380

Vaverka, J., Pellinen-Wannberg, A., Kero, J., Mann, I., De Spiegeleer, A., Hamrin, M., et al. (2017a). Detection of meteoroid hypervelocity impacts on the cluster spacecraft: First results. *Journal of Geophysical Research: Space Physics*, *122*, 6485–6494. https://doi.org/10.1002/2016JA023755

Vaverka, J., Pellinen-Wannberg, A., Kero, J., Mann, I., De Spiegeleer, A., Hamrin, M., et al. (2017b). Potential of earth orbiting spacecraft influenced by meteoroid hypervelocity impacts. *IEEE Transactions on Plasma Science*, *45*(8), 2048–2055.

Wang, Z., Gurnett, D. A., Averkamp, T. F., Persoon, A. M., & Kurth, W. S. (2006). Characteristics of dust particles detected near Saturn's ring plane with the Cassini radio and plasma wave instrument. *Planetary and Space Science*, *54*(9-10), 957–966.

Wood, S. R., Malaspina, D. M., Andersson, L., & Horanyi, M. (2015). Hypervelocity dust impacts on the Wind spacecraft: Correlations between ulysses and wind interstellar dust detections. *Journal of Geophysical Research: Space Physics*, *120*, 7121–7129. https://doi.org/10.1002/2015JA021463

Ye, S., Gurnett, D. A., Kurth, W. S., Averkamp, T. F., Kempf, S., Hsu, H. W., et al. (2014). Properties of dust particles near saturn inferred from voltage pulses induced by dust impacts on Cassini spacecraft. *Journal of Geophysical Research: Space Physics*, *119*, 6294–6312. https://doi.org/10.1002/2014JA020024

Ye, S., Gurnett, D. A., Kurth, W. S., Averkamp, T. F., Morooka, M., Sakai, S., & Wahlund, J. (2014). Electron density inside Enceladus plume inferred from plasma oscillations excited by dust impacts. *Journal of Geophysical Research: Space Physics*, *119*, 3373–3380. https://doi.org/10.1002/2014JA019861

Ye, S., Kurth, W. S., Hospodarsky, G. B., Averkamp, T. F., & Gurnett, D. A. (2016). Dust detection in space using the monopole and dipole electric field antennas. *Journal of Geophysical Research: Space Physics*, *121*, 11,964–11,972. https://doi.org/10.1002/2016JA023266

Ye, S., Kurth, W. S., Hospodarsky, G. B., Persoon, A. M., Sulaiman, A. H., Gurnett, D. A., et al. (2018). Dust observations by the radio and plasma wave science instrument during Cassini's grand finale. *Geophysical Research Letters*, *45*, 10,101–10,109. https://doi.org/10.1029/2018GL078059

Zaslavsky, A. (2015). Floating potential perturbations due to micrometeoroid impacts: Theory and application to S/WAVES data. *Journal of Geophysical Research: Space Physics*, *120*, 855–867. https://doi.org/10.1002/2014JA020635

Zaslavsky, A., Meyer-Vernet, N., Mann, I., Czechowski, A., Issautier, K., Le Chat, G., et al. (2012). Interplanetary dust detection by radio antennas: Mass calibration and fluxes measured by STEREO/WAVES. *Journal of Geophysical Research*, *117*, A05102. https://doi.org/10.1029/2011JA017480